THE ASTROPHYSICAL JOURNAL, 367:54–63, 1991 January 20

HOLLOW GALACTIC HALOS OF FERMIONIC DARK MATTER

JOHN P. RALSTON AND LESLEY L. SMITH
Department of Physics and Astronomy, University of Kansas
Received 1989 December 26; accepted 1990 July 23

ABSTRACT

Fermi statistics and velocity anisotropy give a surprisingly rich structure to massive neutrino dark matter halos. If a spherically symmetric halo has an anisotropic phase space, then hollow halos with a minimum of the mass density at the center are possible. Hollowness of a halo is controlled by a dimensionless constant $K_0 = (g_\nu/4\pi)(m^2/M_p^2)(L_0^2/\hbar^2)(c/[\mu]^{1/2})$ involving the fermion mass, m, the Planck mass M_p, and parameters L_0 and $\mu^{1/2}$ fixing the halo anisotropy. All dependence of a halo on fermion mass and the maximum phase-space density is contained in K_0. For $K_0 \ll 1$, i.e., for small enough fermion mass and effective core size, most halos must be hollow to satisfy Fermi statistics. Thus, existing neutrino lower mass bounds not only are overly restrictive but become inapplicable. It follows that neutrinos or other fermions in the mass range $m \lesssim 100$ eV are viable candidates for galactic dark matter. A flat rotation curve is also shown to be a generic result of anisotropy in the same limit of interest. We discuss observable consequences of the possibility that isolated dwarf galaxies are associated with hollow dark matter halos.

Subject headings: dark matter — elementary particles — galaxies: structure — neutrinos

I. INTRODUCTION

Neutrinos may have a nonzero rest mass. Most modern unified theories predict a neutrino mass which is naturally small compared with the charged lepton mass due to the seesaw mechanism (Yanagida 1979; Gell-Mann, Ramond, and Slansky 1980). The order of the masses is thought to follow that of the leptons, i.e., the tau neutrino should be more massive than the electron neutrino. Current limits from laboratory experiments are that the tau neutrino, the muon, and the electron neutrino have masses less than about 35 MeV, 270 keV, and 20 eV, respectively (Particle Data Group 1988).

Massive neutrinos and the big bang theory lead to a dark matter problem. This is because there must exist a certain cosmological abundance of neutrinos from the big bang. The number density of neutrinos plus antineutrinos ($n_\nu + n_{\bar\nu}$) is directly related to the number density of photons (n_γ) by

$$n_\nu + n_{\bar\nu} = \tfrac{3}{11} n_\gamma \cong 109 \text{ cm}^{-3} .$$

A nonzero neutrino mass implies a nonzero cosmological mass density. Comparing the critical density (ρ_c) needed to close the universe,

$$\rho_c = \frac{3}{8\pi}\frac{H^2}{G} = 1.88 \times 10^{-29} h^2 \text{ g cm}^{-3}$$

with the big bang number density, we obtain a characteristic mass:

$$m_0 = 96.8 \text{ eV} .$$

Since this assumes that one neutrino species dominates the mass, it is an upper bound (Cowsik and McClelland 1972; Schramm and Steigman 1981). It is a profound coincidence that this mass value is in the same range of values permitted for neutrino masses in particle physics.

Even more compelling in the case for neutrinos as dark matter is that the range of masses implied above, say 10 eV $< m <$ 100 eV, also occurs in data for a vast hierarchy of distance scales much smaller than that of the universe. The range of distance scales extends from very large scale structures upward of 100 Mpc to dark matter in the Virgo supercluster to galactic-size halos (Binney and Tremaine 1987; Cowsik and Ghosh 1987).

An independent probe of dark matter, detecting radiative neutrino decay with production of ionizing photons ($E_\gamma > 13.6$ eV), has recently focused attention on the same mass range (Melott, McKay, and Ralston 1988; Ralston, McKay, and Melott 1988; Ralston and McKay 1989; McKay and Ralston 1989; Sciama 1989, 1990). Data indicating an order-of-magnitude excess flux of cosmological ultraviolet photons (Reynolds 1984; Reynolds *et al.* 1986) has, however, recently become controversial (Songaila, Bryant, and Cowie 1989). The most promising test of radiative neutrino decay is the presence of a monochromatic line (DeRujula and Glashow 1980; Stecker 1980).

There are two problems with neutrinos as a sole source of dark matter. One problem involves large-scale structure and galaxy formation, and early claims and arguments that gravitational evolution of neutrinos may or may not be able to produce objects as small as galaxies (Doroshkevich *et al.* 1980). The conclusions have been somewhat controversial and model-dependent and will not be studied here. Analytic arguments (Davis *et al.* 1980; Kaiser 1983) based on large velocity dispersions neglected a substantial population of the low neutrino velocity region. Numerical studies (e.g., White, Frenk, and Davis 1983) seemed to rule out a neutrino-dominated universe. At the same time, other numerical studies (Melott 1983, 1985; Collins, Joseph, and Robertson 1985) showed that galaxy-sized, low velocity dispersion objects could occur in the nonlinear gravitational evolution and comprise of the order of 10% of the total mass. This is the right order of magnitude for galactic dark matter. Moreover, evidence was found for preservation of high phase space density regions, i.e., the absence of substantial phase mixing is not a very rare event (Melott 1983). Finally, changing the spectrum of input fluctuations (e.g., with cosmic strings) affects the conclusions and is another way to encourage galaxy-sized objects to form (Scherrer, Melott, and Bertschinger 1989). The upshot of all this is that neutrino hot

dark matter has certainly not been ruled out and has been gradually regaining popularity.

The other problem involves dwarf galaxies and the constraints from Fermi statistics. It has been proposed that galaxy data could rule out neutrinos as dark matter, at least in isolated dwarf galaxies (Cowsik and McClelland 1973; Tremaine and Gunn 1979; Aaronson 1983; Lin and Faber 1983; Spergel, Weinberg, and Gott 1988). In this paper we will see how such a conclusion does not really follow and that dwarf galaxies might be understood as natural consequences of neutrino dark matter.

Cowsik and McClelland (1973) formulated an early lower bound on the neutrino mass assuming Fermi statistics in the sense that the phase-space density should not be larger than a maximum determined by $\hbar$. Several other authors (Aaronson 1983; Lin and Faber 1983; Madsen and Epstein 1984, 1985) followed the same logic. In these discussions, a neutrino is defined as light, collisionless fermion, so the results apply to any such system. For this paper we summarize the gist of the arguments as follows.

The phase-space density $dN/d^3x\,d^3p$ should be less than that from neutrinos evolving after the big bang,

$$\frac{dN}{d^3x\,d^3p} < \frac{g_\nu}{(2\pi\hbar)^3}\frac{1}{\exp\,(p/kT)+1} < \frac{g_\nu}{2(2\pi\hbar)^3}\,, \tag{1}$$

where g_ν is the number of occupied spin states, $1 < g_\nu < 2$. Note that this density is of the order of the uncertainty principle value using $\Delta^3x\,\Delta^3p \geq \hbar^3$. For an estimate, $dN/d^3x\,d^3p \cong \rho(x)/m^4(\bar{v}^2)^{3/2}$ in order of magnitude, where $\bar{v}^2$ is a characteristic velocity-squared scale in the distribution and $\rho(x)$ is the mass density of neutrinos of mass m. We immediately obtain a bound on m:

$$m^4 > \frac{\rho(x)}{(\bar{v}^2)^{3/2}}\frac{2(2\pi\hbar)^3}{g_\nu}\,. \tag{2}$$

For a dark matter galaxy halo $\rho(x)$ is "measurable," or at least changes of the integral of ρ, the total enclosed mass determining the gravitational field, are measurable with rotation curves. For an order of magnitude it is also plausible (if not rigorous) to relate the velocities of orbiting neutrinos to that of the stars, to estimate $\bar{v}^2$. For example, Tremaine and Gunn (1979) assumed an isothermal sphere neutrino distribution with core size $r_c^2 = 9\sigma^2/4\pi G\rho(0)$ to relate the neutrino velocity distribution to the stellar velocity dispersion $\langle v^2\rangle = \sigma^2$. The Tremaine-Gunn (TG) limit, using this assumption in equation (2), and assuming equal numbers of one species of neutrino and antineutrino, is

$$m^4 \geq m_{\rm TG}^4 = \frac{9\sqrt{2\pi}\,\hbar^3}{2g_\nu r_c^2\,\sigma G}\,;$$
$$m_{\rm TG} = 120\ {\rm eV}\left(\frac{100\ {\rm km\ s^{-1}}}{\sigma}\right)^{1/4}\left(\frac{1\ {\rm kpc}}{r_c}\right)^{1/2} g_\nu^{-1/4}\,. \tag{3}$$

Certain isolated dwarf galaxies have comparatively small values of σ and small core sizes r_c. Recently Spergel, Weinberg, and Gott (1988) observed that the parameters measured for DDO 154 by Carignan and Freeman (1988) imply a value of m that is inconsistent with the upper bound on m due to the flatness of the universe, if equation (3) is taken literally.

It is accepted that the neutrino mass constraint (3) becomes weaker if the neutrino velocities are much larger than the stellar velocities (Cowsik and Ghosh 1986, 1987; Kormendy 1985; Silk 1985). However, if the neutrino rms velocities were as much as 10 times the stellar velocities, the bound is weakened only by a factor of $10^{-1/4} = 0.57$. Another immediate consequence is that the neutrino halos will extend far beyond the stellar system.

The phase-space bounds have loopholes, however. Neutrinos streaming into a halo under formation carry angular momentum. If the system collapses in a roughly spherical way, the angular momentum must be conserved. A collisionless system under such circumstances should generally develop an anisotropic velocity distribution, meaning that some components of the velocity can be much larger than others. This has been known in general for stellar dynamics for some time (Binney 1982; Binney and Tremaine 1987). For neutrinos it follows that the case of large radial velocities—caused by limited angular momentum at the beginning of the halo formation—naturally weakens the neutrino mass bounds by spreading the neutrinos over a larger phase-space volume (Madsen and Epstein 1985; Ralston 1989).

Anisotropy in collisionless self-gravitating systems is not a new subject. Michie (1963) studied anisotropic models for stellar systems some time ago. Kent and Gunn (1982) used a Michie anisotropic model for the dark matter in the Coma Cluster without imposing Fermi statistics. That anisotropy developed in the nonlinear evolution of neutrinos producing galaxy-sized objects was observed in numerical studies by Melott (1983).

One consequence of dark matter velocity anisotropy is rather drastic. Hollow halos can form in which the central density is less than that away from the center. Considering that the angular momentum potential barrier $V_L(r) = L^2/2mr^2$ is more singular than the gravitational attraction, hollow halos for the collisionless system are an obvious possibility. A hollow halo can contain a much greater mass (for the same maximum density) because the highest density occurs in an entire shell. Thus the usual neutrino mass bounds immediately become invalid.

Another unexpected consequence of anisotropy is the truly generic occurrence of a flat rotation curve. Of course, the isothermal sphere also generates acceptable flat rotation curves, and consequently a large number of data have been analyzed assuming an isothermal distribution. But if the isothermal distribution constitutes one acceptable point in the space of all distributions, the anisotropic distribution is an entire subspace, an infinitely larger class. *Any anisotropic distribution of any shape will give a flat rotation curve* provided only that there are cutoffs in the angular momentum and energy ranges. This may explain why nature did not need to conspire to exhibit so many flat rotation curves.

Surprisingly, when Fermi statistics are imposed, we can show that the case of anisotropy and a small neutrino mass *requires* a hollow halo and a flat rotation curve. Thus, it turns out that a hollow fermionic halo is an entirely distinctive object. In relating neutrino velocities to star velocities, relations such as the TG limit (3) might be misapplied. The range of parameters for which hollow halos are implied is the range indicated for isolated dwarf galaxies. We will conclude that if isolated dwarf galaxies are gravitationally dominated by neutrinos, then their dark matter distributions are almost certainly hollow. Indeed, we do not know for sure that normal-size spiral galaxies are *not* hollow.

The paper is organized as follows. Section II reviews the

formalism for collisionless systems and reduces the anisotropic problem to one involving dimensionless variables. The usual dimensional analysis which relates the core size, central density, and velocity dispersion is revised when anisotropy is present. Halos can be classified by a dimensionless constant which is the ratio of two size scales, this ratio being of order unity for the isotropic case. The analysis of a model anisotropic distribution is then presented, and stability of solutions is discussed. Numerical work is presented in § III.

The analysis is complete and self-contained because the concept of a hollow dark matter halo is new. However, readers wishing to preview the general results may wish to skip ahead to § IV, where results are listed.

II. PHASE-SPACE ANISOTROPY

A review of the formalism for collisionless systems is given by Binney and Tremaine (1987). We consider solutions to the Poisson-Vlasov (PV) equation for the velocity-position space distribution $f(\boldsymbol{x}, \boldsymbol{v}) < g_\nu m^3/2(2\pi\hbar)^3$. Solutions obeying this condition will be called Fermi-allowed. The steady state, time-independent solutions are functions of conserved variables, which for spherical symmetry are limited to be the energy per mass $\mathscr{E}$ and the magnitude of the angular momentum L^2:

$$f(\boldsymbol{x}, \boldsymbol{v}) = f(\mathscr{E}, L^2) , \quad \mathscr{E} = \tfrac{1}{2}v^2 + \psi(r) ,$$
$$L^2 = m^2 r^2 v^2 [1 - (\hat{\boldsymbol{v}} \cdot \hat{\boldsymbol{r}})^2] .$$

The number density $n(r)$ is equal to $\int d^3v f(\boldsymbol{x}, \boldsymbol{v})$. We assume spherical symmetry, so that the gravitational potential ψ is a function of the radial coordinate r; $\hat{\boldsymbol{r}}$ is the radial unit vector. Our convention for the zero of $\psi(r)$ will be $\psi(0) = 0$.

The PV equation is

$$\nabla^2\psi = 4\pi G m \int d^3v f(\boldsymbol{x}, \boldsymbol{v}) . \tag{4}$$

Since $f = f(\mathscr{E}(\psi(x), \boldsymbol{v}), L^2)$ to be time-independent, the system is nonlinear and must be treated numerically. Before doing this, we make the following observations to gain some insight into the problem.

a) Dimensional Analysis

First we use dimensional analysis. Dimensionless variables will be denoted by a tilde. From the discussion the natural units of $f(\boldsymbol{x}, \boldsymbol{v})$ are $g_\nu m^3/2(2\pi\hbar)^3$; thus we define

$$f(\boldsymbol{x}, \boldsymbol{v}) = \tilde{f}(\boldsymbol{x}, \boldsymbol{v})/\gamma , \quad \gamma = 2(2\pi\hbar)^3/m^3 g_\nu ,$$
$$n(r) = \frac{1}{\gamma}\int d^3v \tilde{f}(\boldsymbol{x}, \boldsymbol{v}) .$$

The mass density $\rho(r) = mn(r)$ can be written $\rho = \rho_0\tilde{\rho}$, where $\tilde{\rho}$ is dimensionless. Letting the velocity-squared in the distribution range up to a value 2μ, the natural size of ρ_0 is $\pi\mu^{3/2}m/\gamma$. Here we have dropped a factor of $2^{7/2}/3$ in the volume of the velocity sphere to simplify definitions. We use the symbol μ rather than σ^2 to emphasize the distinction between the neutrino velocities and gas or star velocities measured in rotation curves. The units of ψ are velocity-squared, conveniently expressed in units of μ. The PV equation of such a dimensionless variable is

$$\nabla^2\left[\frac{\psi(r)}{\mu}\right] = \frac{4\pi G\rho_0}{\mu}\tilde{\rho}(r) .$$

Dimensional analysis dictates that the constant $\mu/4\pi G\rho_0$ in this equation sets a squared-distance scale of the halo. This is exactly as in the isothermal sphere, where the "core size" $r_c^2 = 9\sigma^2/4\pi G\rho(0)$. For any isotropic distribution, the same type of dimensional analysis applies. The dominance of dimensional analysis explains why there is not much difference between the neutrino mass bounds for the isothermal sphere and other isotropic distributions.

On the other hand, an anisotropic halo has *two* independent scale sizes: the usual core size and an impact parameter size scale. Let L_0^2 be an angular momentum scale in the distribution, i.e., $f(\boldsymbol{x}, \boldsymbol{v}) = f(\mathscr{E}, L^2/L_0^2)$. The presence of L_0^2 is equivalent to the presence of the impact parameter scale a, with $L_0 = m(\mu)^{1/2}a$. A natural dimensionless unit of distance will be $\tilde{r} = r/a$. The dimensionless PV equation for anisotropically distributed fermions is

$$\tilde{\nabla}^2\tilde{\psi}(\tilde{r}) = K_0\tilde{\rho}(\tilde{r}) ,$$
$$\tilde{\psi} = \frac{\psi}{\mu} , \quad \tilde{\nabla}^2 = a^2\nabla^2 , \quad \tilde{\rho} = \frac{\rho}{\rho_0} ; \quad K_0 = \frac{4\pi G L_0^2\rho_0}{\mu^2 m^2} .$$

Evidently the dimensionless constant K_0 plays a decisive role in the PV equation for fermions. If we ignore the distinction between stellar and neutrino velocity dispersions, then, to order of magnitude, $K_0 \cong a^2/r_c^2$. Consequently K_0 will be called the scale ratio. In any situation where K_0 is much different from unity, isothermal sphere physics is liable to be misapplied.

K_0 depends on quantum mechanics through Planck's constant. With no approximations K_0 may be written

$$K_0 = \frac{g_\nu}{4\pi}\frac{L_0^2}{\hbar^2}\frac{m^2}{M_p^2}\frac{c}{\mu^{1/2}} ,$$

where $M_p = (\hbar c/G)^{1/2} = 1.22 \times 10^{19}$ GeV is the Planck mass. For a numerical estimate of K_0 using $m = 30$ eV, we consider a normal galaxy, where stellar rotation curves give us apparent velocities $\mu^{1/2} \simeq 300$ km s^{-1} and apparent core sizes $a \cong 10$ kpc, so $L_0 = m(\mu)^{1/2}a \cong 4.7 \times 10^{25}\hbar$. These are typical values (Kormendy 1985; Rubin 1985). Putting all the factors together, one finds

$$K_0 = 1.06 g_\nu \left(\frac{L_0}{4.7 \times 10^{25}\hbar}\right)^2\left(\frac{m}{30 \text{ eV}}\right)^2\left(\frac{300 \text{ km s}^{-1}}{\mu^{1/2}}\right) .$$

The cancellation of large numbers above to give K_0 of order unity for a normal galaxy cannot be ignored. Turning the relations around, the condition $K_0 \simeq 1$ so that the core size equals the impact parameter allows us to calculate a typical galactic core size (10 kpc). This is the conventional result of isotropy, and another enormous coincidence of neutrino dark matter.

There is an intimate relation between the scale ratio K_0 and the usual phase-space mass bounds. Let $m_{\rm TG}$ be the maximum neutrino mass with the usual isothermal sphere assumptions (3); m is the actual neutrino mass. Eliminating constants in equation (3), one obtains a revised bound:

$$m^4 > 0.56\frac{\sigma}{\mu^{1/2}}\frac{r_c^2}{a^2}K_0 m_{\rm TG}^4 . \tag{5}$$

Now, even retaining the usual assumption that the neutrino and stellar velocities are comparable, $\sigma/\mu^{1/2} \cong 1$, and assigning the ratio $r_c/a \cong 1$, the mass bound is drastically weakened if $K_0 \ll 1$. (Numerical work in § III will demonstrate that scaling halos in units of a is the natural choice. Many halos over a wide range of K_0 still have comparable core sizes in these

units.) Put another way, the revised bound says that if we already know $m^4 \ll m_{TG}^4$, then we should study halos with $K_0 \ll 1$.

We will see below that hollowness of a Fermi-allowed solution to the PV equation occurs when K_0 is small compared with unity. Dwarf galaxies are small, so we expect the angular momentum scale L_0 to be small, and $K_0 \ll 1$ is indicated. For example, reducing the core size a to 1 kpc and apparent velocity $\mu^{1/2}$ to 30 km s^{-1}, we find $K_0 \simeq 10^{-3}$ for neutrino mass $m = 30$ eV. Note that we anticipate $K_0 \ll 1$ for a normal galaxy if the neutrino mass is much smaller than 30 eV. Consequently we concentrate on the cases $K_0 \ll 1$ and $K_0 \approx 1$ in this paper.

b) *The Momentum Tensor*

Returning to the PV equation, if it is solved we automatically solve the Jeans equations for hydrostatic equilibrium:

$$\frac{\partial}{\partial r}(\rho\langle v_r^2\rangle) + \frac{\rho}{r}(2\langle v_r^2\rangle - \langle v_\vartheta\rangle^2 - \langle v_\varphi^2\rangle) = -\frac{GM(r)\rho(r)}{r^2} . \quad (6)$$

Here $(v_r, v_\vartheta, v_\varphi)$ are the velocity components in spherical coordinates, and $\langle v_r^2\rangle = \int d^3v\, v_r^2 f(\boldsymbol{x}, \boldsymbol{v})/n(r)$, etc. Properties of the Jeans equations can tell us properties of the Poisson-Vlasov system. We focus on the effects of anisotropy, $\langle v_r^2\rangle \neq \langle v_\vartheta^2\rangle$, while $\langle v_\vartheta^2\rangle = \langle v_\varphi^2\rangle$ from symmetry. First note that the term going as $2\langle v_r^2\rangle - \langle v_\vartheta^2\rangle - \langle v_\varphi^2\rangle$ represents an extra centrifugal force density. Expanding equation (6) around $r = 0$, we find some conditions for solutions to exist (Ralston 1989). The conditions are most simply expressed in terms of momentum tensor components $T_\parallel$, $T_\perp$,

$$T_\parallel(r) = \rho(r)\langle v_r^2(r)\rangle , \quad T_\perp(r) = \tfrac{1}{2}\rho(r)(\langle v_\vartheta^2\rangle + \langle v_\varphi^2\rangle) .$$

Together these form the most general spherically symmetric momentum tensor $T_{ij} = T_\parallel \hat{\boldsymbol{r}}_i\hat{\boldsymbol{r}}_j + T_\perp(\delta_{ij} - \hat{\boldsymbol{r}}_i\hat{\boldsymbol{r}}_j)$. Expanding

$$T_\parallel(r) = T_\parallel(0) + rT'_\parallel(0) + \frac{r^2}{2}T''_\parallel(0) ,$$

$$T_\perp(r) = T_\perp(0) + rT'_\perp(0) + \frac{r^2}{2}T''_\perp(0) ,$$

we find that equation (6) is satisfied only if the following conditions are met:

$$T_\perp(0) = T_\parallel(0) , \quad T'_\perp(0) = (\tfrac{3}{2})T'_\parallel(0) ,$$
$$T''_\perp(0) = 2T''_\parallel(0) + 4\pi G\rho^2(0)/3 .$$

The first relation above shows that if T_{ij} is finite at the center, then it must be isotropic. However, if $T_\parallel(0) = T_\perp(0) = 0$, then there is no need for isotropy. Put another way, if the distribution is anisotropic, then either we have zero central density or the distribution becomes isotropic at the center. The relation between the first derivatives shows that the origin can then be a minimum of the momentum tensor. For reasonable distributions this is tantamount to a local minimum of the density at the center.

For a hollow halo we need $T_\parallel > T_\perp$ in a large enough region to give $\partial\rho/\partial r > 0$. After reaching a maximum value, ρ will then decrease as the gravitational attraction overcomes the centrifugal barrier (Ralston 1989). Recently Madsen (1989) has studied hollow solutions to the Jeans equations (6) assuming an anisotropic Fermi ellipsoid equation of state. This and other work with similar assumptions (Madsen and Epstein 1984, 1985) will generally not satisfy the PV equation and therefore will give a time-dependent halo which may be of interest for other purposes.

c) *Hollowness*

We can learn more by examining the expansion of the PV equation near the origin. In this paper we comsider distributions of the form

$$f(\mathscr{E}, L^2) = f(\mathscr{E})g(L^2/L_0^2) . \quad (7)$$

Isotropic distributions are the special case $g(L^2/L_0^2) =$ constant. For the case of physical interest we have already assumed that $\mathscr{E}$ ranges up to some maximum μ in the distribution, with a fairly sharp cutoff. A specific example (physically motivated below) is $f(\mathscr{E}) = \vartheta(\mu - \mathscr{E})$. Other examples would be any strongly damped function of $\mathscr{E}/\mu$. The following observations apply to any such cutoff distribution.

As $r \to 0$, $g(L^2)$ for $L^2 \to 0$ dominates the physics. This is because $\mathscr{E} = \frac{1}{2}v_r^2 + \frac{1}{2}L^2/m^2r^2 + \psi \lesssim \mu$ requires L^2 to be small: $L^2 \lesssim 2\mu m^2 r^2$ to permit any volume in velocity space. Thus $g(0)$ and its derivative $g'(0)$ determine the character of the density $n(r)$ and the momentum tensor $T_{ij}(r)$ near $r = 0$.

To make this quantitative, we expand

$$f(\mathscr{E}, L^2/L_0^2) = \vartheta(\mu - \mathscr{E})[g(0) + g'(0)L^2 + g''(0)L^4/2!] \quad (8)$$

and calculate $n(r)$. The result, after a certain amount of integration and algebra, is

$$n(r) = \frac{4\pi}{3}(2\mu)^{3/2}g(0) + 2^{5/2}\pi\mu^{3/2} \times\left[\frac{8}{15}g'(0)m^2\mu - \frac{2^{9/2}}{9}\pi^2 Gm(\mu)^{1/2}g^2(0)\right]r^2 + O(r^4) . \quad (9)$$

Thus the expansion of $n(r)$ is coupled to the expansion of $g(L^2)$. In deriving this, the potential $\psi(r)$ has been expanded with the boundary conditions $\psi(0) = \psi'(0) = 0$, and its second derivative has been eliminated using $\nabla^2\psi(r) = 4\pi G\rho(r)$.

From equation (9) we see that if $g(0) = 0$, then $n(0) = 0$, i.e., we have a solution with zero central density. Conversely, if $g(0) \neq 0$, then the central density is finite. Next, if $n''(0) > 0$, then the density increases with r near $r = 0$. The condition of $n''(0) > 0$ gives a condition on $g'(0)$ in terms of $g^2(0)$:

$$g'(0) > \frac{\alpha g^2(0)G}{m(\mu)^{1/2}} , \quad (10)$$

with $\alpha = 10\sqrt{2}\pi^2/3$. When this inequality is satisfied, we have a hollow halo. The factors contributing to inequality (10) are of rather general origin, so formula (10) applies as a criterion to any factored distribution (7) with a finite range of energies per mass $\mathscr{E} \lesssim \mu$, allowing α to be varied somewhat for a particular distribution.

The hollowness condition (10) has the following interpretation. Dividing by $g(0)$, on the left-hand side the logarithmic derivative $\partial \ln g(0)/\partial L^2$ represents a typical inverse angular momentum scale in the distribution. In an order-of-magnitude estimate this scale can be identified with $1/L_0^2$. On the right-hand side $g(0)$ carries the dimensions of the distribution, which to order of magnitude is $1/\gamma$. Thus, from formula (10), the halo is hollow if

$$\frac{\alpha G m^2 L_0^2}{2(2\pi)^3\hbar^3(\mu)^{1/2}} \lesssim 1 .$$

The combination on the left-hand side above is $(5/3\sqrt{2})K_0 = 1.18K_0$. We conclude that $K_0 \lesssim 1$ determines that a halo is hollow. This is rather general, allowing for some variation in the critical value of K_0 for particular distributions.

The details of a particular distribution do have an effect in determining the critical value of K_0 for hollowness. The family of functions we study numerically is given by

$$g\left(\frac{L^2}{L_0^2}\right) = \frac{1}{\gamma}\left(A\,\frac{L^2}{L_0^2} + B\right)\exp\left(-\frac{L^2}{2L_0^2}\right), \tag{11}$$

where A, B, and L_0^2 are parameters.

We demand that the phase-space density be consistent with Fermi statistics (eq. [1]). Finding the maximum of $g(L^2)$ in equation (11), which coincides with the maximum of $f(\mathscr{E}, L^2)$ for the cases we study, and imposing Fermi statistics with

$$g(L^2/L_0^2) \le 1/\gamma\,,$$

we obtain conditions on A and B:

$$\begin{aligned} 2Ae^{B/2A-1} &\le 1\,, \quad B < 2A\,, \\ B &\le 1\,, \quad B > 2A\,. \end{aligned} \tag{12}$$

Solving for B, Fermi statistics requires

$$\begin{aligned} B &\le 2A[1 - \ln(2A)]\,, \quad A > \tfrac{1}{2}\,, \\ &\le 1\,, \qquad\qquad\quad 0 < A < \tfrac{1}{2}\,. \end{aligned} \tag{13}$$

Next we examine hollowness. Using equations (10) and (11), the halo is hollow if $K(A, B) < 1$, where

$$\begin{aligned} K(A, B) &= \frac{B^2}{A - B/2}\,\frac{\alpha G L_0^2}{m(\mu)^{1/2}\gamma}\,, \quad B < 2A\,, \\ &= \frac{B^2}{A - B/2}\,\frac{5}{3\sqrt{2}}\,K_0\,. \end{aligned} \tag{14}$$

Combining equations (13) and (14), we can classify halos. All neutrino halos must satisfy equations (13); the subset satisfying $K(A, B) < 1$ are hollow. There is also the case of $B \ge 2A$ which is not hollow for any K_0. The results are shown graphically in Figure 1.

In the figure, parameters B and A satisfying Fermi statistics (eqs. [13]) lie in the region of positive values below the solid curve. Also shown in dashed lines are curves of constant $K(A, B) = 1$ for different fixed values of K_0. The region of B and A values below each dashed curve corresponds to $K(A, B) < 1$ or hollow halos, and those above the curve to $K(A, B) > 1$. Note that if $K_0 \ll 1$, then most of the Fermi-allowed region lies below the dashed curve, so almost all of the halos are hollow. (In the limit $K_0 \to 0$ the dashed curves approach the line $B = 2A$.) For $K_0 \gtrsim 1$, the dashed curve cuts through the Fermi-allowed region, dividing it into sectors of halos which are hollow and those that are not. Again, $K_0 \approx 1$ is a critical value for Fermi-allowed halos.

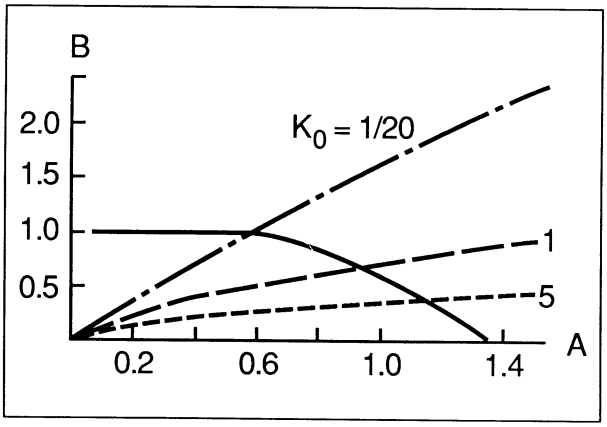

FIG. 1.—Space of parameters A and B describing the halo anisotropy (eq. [11]). Fermi-allowed halos have A and B positive and below the solid line. Dashed curves determine hollowness. For fixed values of K_0 shown, parameters A and B below each dashed curve give hollow halos. For $K_0 \lesssim 1$ most Fermi-allowed halos are hollow.

For parameter $A < \frac{1}{2}$ the phase-space distribution has its maximum at $L = 0$; for $A > \frac{1}{2}$ the maximum point is away from $L = 0$. Maximal halos, i.e., the maximum density allowed by Fermi statistics, correspond to equality in equations (13) and the solid line in Figure 1. The plots show the effect of parameter A, which controls the location of the peak in the angular momentum distribution. The case $A = 1.3$ is close to the limiting value $A = e/2$ that gives the most hollow halo [$\rho(0) = 0$]; the case $A = 0.3$ is a nonhollow halo for any K_0. Numerical work presented below will study several cases: $A = 0.3$, 1.0, and 1.3.

d) Asymptotic Behavior

Data on dark matter in galactic halos show nominally flat rotation curves. This occurs both in the more easily studied spiral galaxies and in dwarf galaxies (Kormendy 1985; Rubin 1985). Consequently, the isothermal sphere, in which a flat rotation curve arises as a detailed nonlinear special effect, has dominated discussions of dark matter. The isothermal sphere is not a realistic model because it has infinite mass and is perfectly isotropic. Under what circumstances will an anisotropic phase-space distribution give a flat rotation curve?

In the region where the rotation curve is flat, the number density $n(r)$ goes roughly as $1/r^2$. This is an approximate behavior over some large but finite region.

Thus we consider the large-r behavior of

$$n(x) = \int d^3v f(\boldsymbol{x}, \boldsymbol{v})\,,$$

$$n(r) = (\pi/m^2r^2)\int dv_r\, dL^2 f(\mathscr{E}, L^2/L_0^2)\,.$$

Here we have used the Jeans theorem and assumed spherical symmetry, orienting cylindrical coordinates in velocity space along $\hat{\boldsymbol{r}}$. Evidently the statement that $n(r)$ goes as $1/r^2$ is equivalent to the integral above being slowly varying in r.

Again we assume that the range of $\mathscr{E}$ is cut off, $\mathscr{E} \lesssim \mu$, and with anisotropy the range of L is cut off, $L^2 \lesssim L_0^2$. We wish to study the generic behavior of such distributions. Dropping constant factors, the density goes as

$$\begin{aligned} n(r) &\sim \frac{1}{r^2}\int dv_r\, dL^2\, \vartheta\left\{v_r^2 + \frac{L^2}{m^2r^2} \lesssim 2[\mu - \psi(r)]\right\}\vartheta(L^2 \lesssim L_0^2) \\ &\sim \frac{1}{r^2}\int dL^2\left[2(\mu - \psi) - \frac{L^2}{m^2r^2}\right]^{1/2}\vartheta(L^2 < L_0^2)\,. \end{aligned}$$

The square root allows L^2 to range up to as much as $2m^2r^2[\mu - \psi(r)]$. For example, near the origin where $\psi \approx 0$ the L^2 integral could give us a contribution going as r^2, giving a constant density. This accounts for the complicated behavior

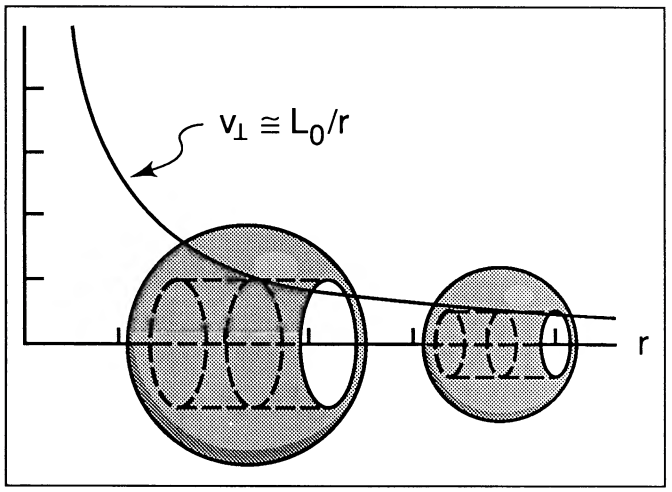

FIG. 2.—Cylindrical plug argument that an angular momentum cutoff and energy cutoff give a flat circular velocity curve. The figure shows the velocity volume $v^2 \lesssim 2[\mu - \psi(r)]$ as spheres at different radii r in coordinate space. The angular momentum $L^2 = m^2 v_\perp^2 r^2 \lesssim L_0^2$ constrains the transverse velocity $v_\perp$ to be within the cylindrical plugs cut inside the spheres. The angular momentum constraint forces the diameter of each plug to decrease as L_0/r. The number density, which is the allowed velocity space volume, goes as the volume of the plugs, i.e., $1/r^2$ for $[\mu - \psi(r)]^{1/2}$ slowly varying. A $1/r^2$ density gives a flat rotation curve.

of the nonlinear problem in the central region. The L^2 cutoff L_0^2 is not important in this region; $2m^2r^2[\mu - \psi(r)] \lesssim L_0^2$.

For large r^2, any L^2 cutoff simplifies the problem considerably. For $2m^2r^2(\mu - \psi) \gtrsim L_0^2$ we can ignore the L dependence in the square root. There is a generic factorization (Ralston 1989):

$$n(r) \sim \frac{1}{r^2}\,[2(\mu - \psi)]^{1/2} \int_0^{L_0{}^2} dL^2 \,.$$

Thus, anisotropy generates a rather flat rotation curve, if only $[\mu - \psi(r)]^{1/2}$ is slowly varying. The region of interest is large r, where $L < L_0$ is being "restricted" below its typical isotropic value $mr(\mu - \psi)^{1/2}$.

This simple result can be understood in a simple way. In Figure 2 the velocity space is sketched at several points in coordinate space. The neutrino mass density goes as the volume of the velocity space. Thus the figure shows a series of spheres for the energy cutoff condition $\mathscr{E} < \mu$, or $v^2 < 2(\mu - \psi)$. The volume of the spheres is fairly constant as ψ is slowly varying. The figure also shows the angular momentum cutoff $L^2 < L_0^2$, which means the transverse velocity $v_\vartheta^2 + v_\varphi^2 < L_0^2/m^2r^2$. This constraint can be represented inside each sphere as cylindrical plugs of diameter going as L_0/r. Evidently the velocity volume allowed by both constraints goes as the plug's length $(\mu - \psi)^{1/2}$ times its cross-sectional area, $\pi L_0^2/m^2r^2$, which gives a density that goes as $1/r^2$. This density implies a flat rotation curve.

We now turn to the spatial variation of $[\mu - \psi(r)]^{1/2}$, assumed to be slow above, but really a self-consistency issue. Suppose $K_0 \ll 1$. The dimensionless PV equation,

$$\tilde{\nabla}^2\tilde{\psi} = K_0\tilde{\rho}\,,$$

where $\tilde{\psi} = \psi/\mu$, shows that the scale ratio K_0 acts somewhat like Newton's constant. The potential $\tilde{\psi}$ grows from zero at $r = 0$ in proportion to the size of $\tilde{\rho}$ and K_0. The size of $\tilde{\rho}$ is of order unity owing to the choice earlier of the largest velocity volume scale ($\rho_0 = \pi\mu^{3/2}m/\gamma$). Thus small K_0 forces small $\tilde{\psi}$. It will be a good approximation to think of $(\mu - \psi)^{1/2} = \mu(1 - \tilde{\psi})^{1/2}$ as slowly varying.

To add detail to this, from $n(r) \sim 1/r^2$ we know $\tilde{\psi} \sim K_0 \ln\tilde{r}$. Thus $\tilde{\psi}$ is not only small, because $K_0 \ll 1$, but it remains small over many units of r/a because it only varies logarithmically.

Thus we see that a rather long, flat rotation curve is a kinematic effect of an anisotropic halo with $K_0 \ll 1$. Anisotropy alone generates $n(r) \sim 1/r^2$ provided that the cutoff L_0^2 dominates the integrals; $K_0 \ll 1$ guarantees that the other factors are slowly varying over a large region. The behavior is mainly of geometrical origin. The numerical work presented below (§ III) confirms this analysis and also gives counterexamples (the case $K_0 \gg 1$). N-body numerical simulations of halo formation (Dobyns 1988) also generally show velocity anisotropy and a behavior for $n(r)$ close to $1/r^2$, but the simple connection seems to have gone unnoticed.

We remark that the region over which $n(r) \sim 1/r^2$ is finite, unlike the isothermal sphere. Provided that there is a cutoff $\mathscr{E} \lesssim \mu$ in the halo, the largest extent of the halo can be found thus: at the outer halo edge r_*, $\psi(r_*) = \mu$ occurs, leaving no phase space and forcing $n(r_*) = 0$. This is an outer Fermi radius where the potential energy is μ. The $1/r^2$ behavior is not a good approximation when r becomes so large that $\psi(r) \cong \mu - L_0^2/2m^2r^2$. Thus the inner core and outer edge of an anisotropic halo are determined by nonlinear effects, which require a numerical treatment, while $K_0 \ll 1$ guarantees a long intermediate region with a flat rotation curve. We do not present results here on the halo edge value r_* versus K_0, which would determine the total halo mass. This project requires slightly more sophisticated numerical work in the extrapolation of small $\tilde{\rho}$ over many units of $\tilde{r}$ than the present numerical method allows. It will be studied elsewhere.

e) *Stability*

It is easy to verify that our distributions (eqs. [7] and [15]) give halos that are stable under the Antonov tests (Antonov 1962; Binney and Tremaine 1987) when applied to distributions of the form $f(\mathscr{E}, L)$. This shows stability under general radial perturbations. However, no systematic method exists for studying the stability of collisionless systems to nonradial perturbations.

In spite of extensive investigation (Fridman and Polyachenko 1984), the general problem of stability has not been resolved analytically. A certain (Fridman and Polyachenko 1984) criterion for stability has been shown to be invalid by a counterexample (Palmer and Papaloizou 1987). Numerical studies (Merritt and Aguilar 1985; Barnes 1986) have demonstrated some radial-orbit instability in some highly anisotropic models of stars in galaxies. Since encounters between stars give a big perturbation that does not occur for neutrinos, the studies do not really apply, but they do show that a particular instability might exist.

We note that the models previously studied have been solid anisotropic halos, which we have seen are in the minority for $K_0 \ll 1$. Since there is more "function space" with hollow halos, it is not too surprising that the privileged solid anisotropic halos might sometimes be found to be unstable.

More physically, consider the origin of radial orbit instability. A particle on a radial orbit and far from the center can receive the smallest sideways "kick" to its velocity, but gain large angular momentum. On its next pass the angular momentum barrier will keep a particle away from the density

peak at the center of a conventional solid halo. One might expect such a perturbation to grow, producing a barlike or triaxial instability that moves density away from the center. The growth of barlike instabilities has recently been discussed by Lynden-Bell (1979).

On the other hand, if there is already considerable density away from the center, as in a hollow halo, then the fractional density perturbation $\delta\rho/\rho$ is naturally smaller in effect. A particle kicked sideways far from the center simply enters the stream of those other particles already present. Thus, it is interesting to speculate that a hollow halo might be a planned superposition of instabilities creating a form that is itself naturally stable. This speculation is beyond the scope of this work, but it might be checked with N-body codes. Care is needed in such checks, because one must be able to watch the system for a long time, and because pointlike encounters must be eliminated properly.

III. NUMERICAL WORK

Here we study the properties of numerical solutions to the PV equation (4). For the anisotropic phase-space distribution we use the factored form (7) with

$$f(\mathscr{E}, L^2) = f(\mathscr{E}) g\left(\frac{L^2}{L_0^2}\right),$$

$$f(\mathscr{E}) = \frac{1}{1 + \exp\left[\beta(\mathscr{E} - \mu)\right]}, \tag{15}$$

and $g(L^2/L_0^2)$ as given by equation (11). The motivation for equations (15) describing fermions should be obvious. We take parameters $\beta\mu \gg 1$, so that equations (15) correspond to the degenerate situation $f(\mathscr{E}) \simeq \vartheta(\mu - \mathscr{E})$. Thus μ is the Fermi energy per mass.

In Figures 3–5 we show the numerical results of maximal Fermi-allowed halos, where $B = 2A[1 - \ln(2A)]$. With B eliminated the halos are functions of A and K_0. We study both hollow and nonhollow halos. In each figure, A is fixed, and halos for different values of K_0 are plotted. $K_0 \gg 1$ corresponds to an isotropic degenerate Fermi phase space $L_0 \to \infty$. Not surprisingly, halos of large K_0 are more compact: recall that K_0 acts somewhat like Newton's constant. The case of small K_0, which corresponds either to small m^2, small L_0^2, large μ, or a combination of these (recall eq. [5]), gives a rather extended halo with a long region of rather flat rotation curve. This confirms the analytic argument of § II*d*. As A is varied, the conditions for a hollow halo change according to equation (14) and Figure 2. The case $A = 0.3$, a nonhollow halo, can be compared with the rather hollow case $A = 1.3$.

Rotation curves are plotted in Figures 3*b*, 4*b*, and 5*b*. We have plotted the circular velocity v_c in dimensionless form, defining $\tilde{v}_c = v_c/\mu^{1/2}$. Then

$$\tilde{v}_c = \left(\frac{K_0}{4\pi}\right)^{1/2}\left[\frac{\tilde{M}(\tilde{r})}{\tilde{r}}\right]^{1/2},$$

where the enclosed mass $M(r)$ is equal to $\int_0^r d^3x\,\rho(r)$ has been eliminated by $M(r) = \rho_0 a^3 \tilde{M}(\tilde{r})$. Note that K_0 controls $\tilde{v}_c$, so that, all other things being equal, halos with smaller K_0 have smaller circular velocities. (To avoid misunderstanding, we remark that in general $\mu^{1/2}$ and K_0 are independent.) The curves show that in the case $K_0 \ll 1$, there is a wide region over which the rotation curve is nominally flat. The rotation curves for nonhollow ($A = 0.3$) and hollow halos ($A = 1.3$) are similar for $K_0 \ll 1$, differing in shape only in the core region. The nonhollow halo with $K_0 \ll 1$ is a generalization of a case of radial orbits considered before (Ralston 1989), giving flat rotation curves. The large r/a dependence of the density, shown in Figure 6*a* in a logarithmic plot, displays the similar power-law decrease for the hollow or nonhollow halos with small K_0. Fixing $K_0 = 1/20$, the rotation curves for hollow and nonhollow halos are compared in Figure 6*b*. More mass is contained in a hollow halo at large radius because the point of maximum density is farther from the center; thus $\tilde{v}_c$ is larger.

The flat rotation curves for $K_0 \ll 1$ suggest that this case may be applicable to data for dwarf galaxy rotation curves. Indeed, the variety of the curves for $K_0 = 1/20$ and different A parameters is strongly reminiscent of the type I, II, and III dark matter halo classifications observed empirically by Rubin (1985). A thorough job of curve fitting also requires informa-

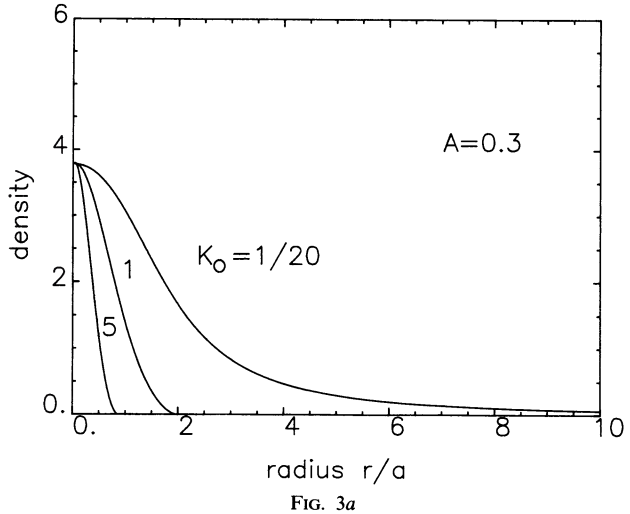

FIG. 3*a*

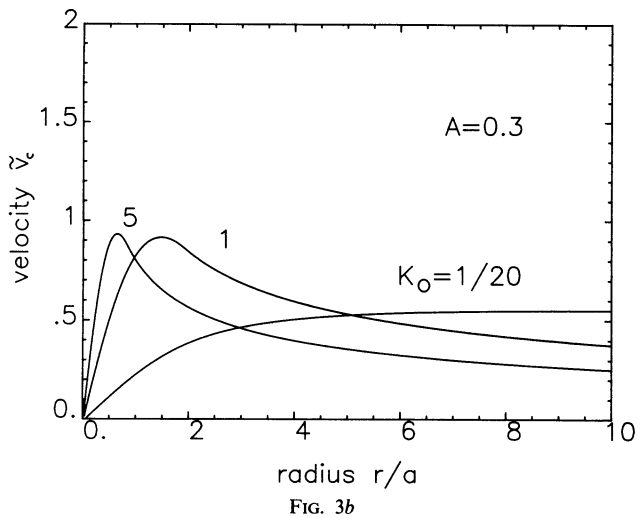

FIG. 3*b*

FIG. 3.—Mass density and circular velocity curves vs. scaled radius for maximal Fermi-allowed halos. (*a*) Curves show the scaled density $\rho(r)/\rho_0$ vs. $\tilde{r} = r/a$ for $K_0 = 1/20$, 1, and 5 and $A = 0.3$. (*b*) Scaled circular velocities $\tilde{v}_c = v_c/\mu^{1/2}$ vs. $\tilde{r}$ for $A = 0.3$ and $K_0 = 1/20$, 1, and 5. The circular velocity curves are nominally flat for $K_0 = 1/20$.

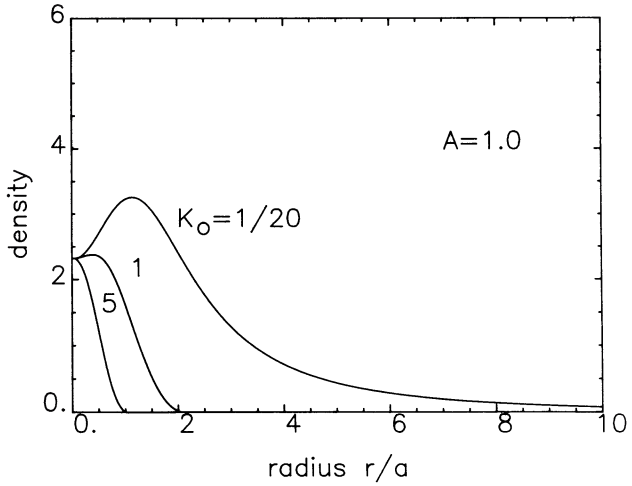

FIG. 4*a*

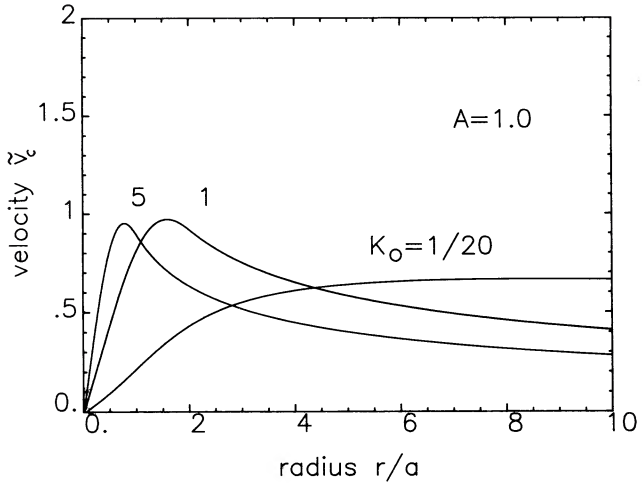

FIG. 4*b*

FIG. 4.—Same as Fig. 3, but for $A = 1.0$

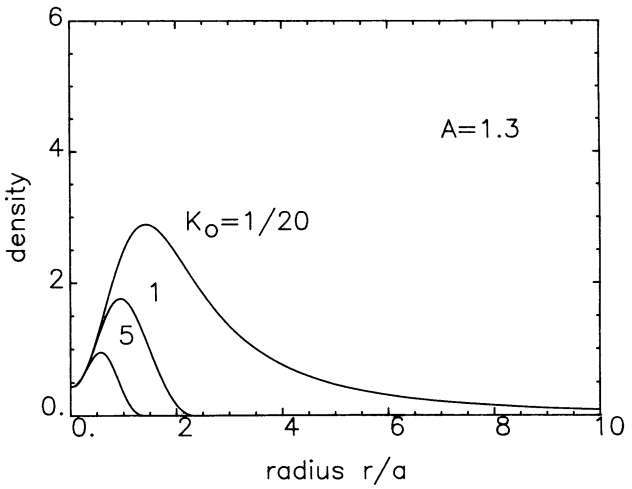

FIG. 5*a*

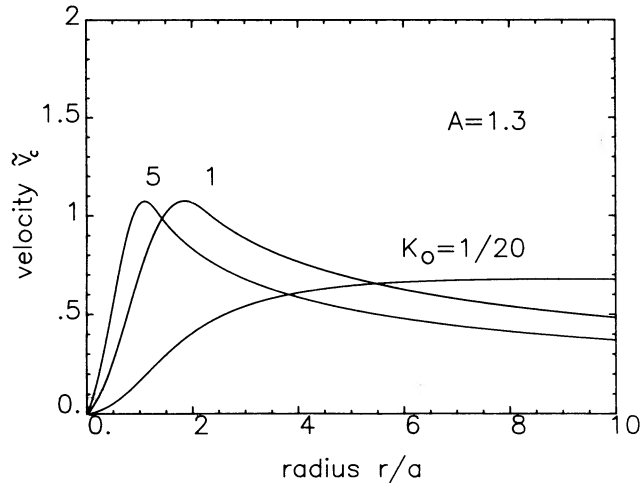

FIG. 5*b*

FIG. 5.—Same as Fig. 3, but for $A = 1.3$

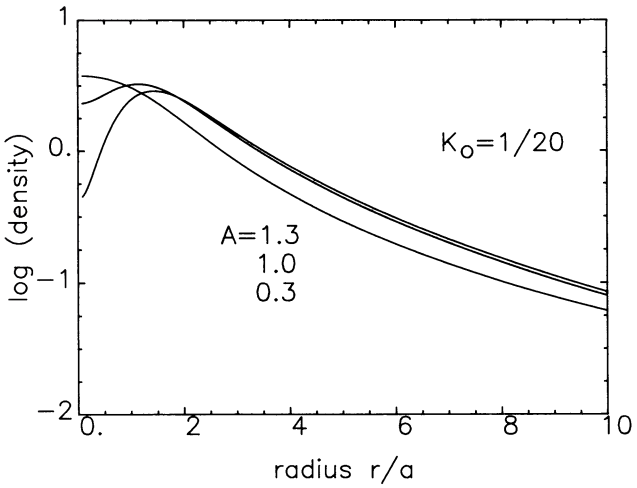

FIG. 6*a*

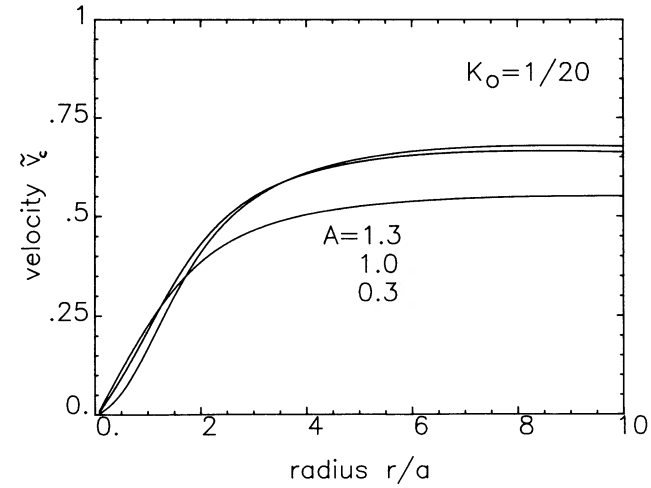

FIG. 6*b*

FIG. 6.—(*a*) Logarithmic plots of the density profiles of halos with different A-values and $K_0 = 1/20$. The dependence of the density at large r is similar for hollow and nonhollow halos. (*b*) Circular velocity curves for $K_0 = 1/20$ and various values of A as shown. For $K_0 \ll 1$, a flat rotation curve is obtained for large r/a regardless of the hollow ($A = 1.0, 1.3$) or nonhollow ($A = 0.3$) behavior of the density near the origin.

tion on dynamical autonomy (Aaronson 1983; Kuhn and Miller 1989) and a detailed model of the visible matter distribution (Kormendy 1985), and is not the purpose of this paper. Instead the curves provide "existence proofs" that a halo of given core size can be made for a given neutrino mass. If m and a are held fixed, $K_0 \ll 1$ requires a small Fermi velocity $\mu^{1/2}$. If m and L_0 are fixed, then $K_0 \ll 1$ requires a large $\mu^{1/2}$, the case studied in less generality earlier (Ralston 1989). Since K_0 contains so much information in a dimensionless form, care must be used to take limits such as these in a physically realistic manner.

To investigate the distribution of observable stars or gas moving in an anisotropic halo, the following procedure was used. Assume that the gas or stars have an isothermal distribution $f(\mathscr{E}_{\rm gas}) \sim \exp(-\beta_g \mathscr{E}_{\rm gas})$. Then if the dark matter dominates, the gas number density $n_g \approx \exp(-\beta_g \mu\tilde{\psi})$. For the neutrinos we have already assumed $\beta\mu \gg 1$, i.e., the Fermi energy is larger than the temperature. Since it seems reasonable to study $\beta_g \simeq \beta$, we set $\beta_g \mu = 10$ and plot $n_g(r)/n_g(0)$ in Figure 7 for various cases: $A = 0.3$, 1.0, and 1.3 with $K_0 = 1/20$. This is a preliminary test that shows that the hollow halos will have the capability of fitting data for the luminous core. This, and the range of parameters K_0, etc., that will fit the data, will be investigated further elsewhere.

IV. DISCUSSION

There are several significant results of this work:

1. A dimensionless constant, the scale ratio K_0, is of decisive importance in fixing the configuration of a Fermi-allowed halo. The constant K_0 is defined by

$$K_0 = \frac{g_\nu}{4\pi}\frac{L_0^2}{\hbar^2}\frac{m^2}{M_{\rm P}^2}\frac{c}{\mu^{1/2}}.$$

K_0 summarizes all dependence of the halo on the neutrino mass m (in units of the Planck mass $M_{\rm P}$), the neutrino Fermi velocity scale $\mu^{1/2}$, and the angular momentum scale of the halo L_0^2.

2. The case $K_0 \ll 1$ tends to give a hollow halo. This was shown by expanding the PV equations near the origin. It is confirmed by numerical work studying a family of distributions (eq. [11]) as shown in Figures 3*a*, 4*a*, and 5*a*.

3. For the entire region where the growth of the potential ψ is slow, a nominally flat rotation curve generically comes from a cutoff in the large-L behavior of the angular momentum distribution. The analysis of § II*d* (Fig. 2) shows this in some generality. The limit $K_0 \ll 1$ is the limit where the L_0 cutoff is small and the growth of $\psi(r)$ is slow, extending the region of flat rotation curve (Figs. 3*b*, 4*b*, and 5*b*; Fig. 6).

4. Phase-space bounds such as the TG bound apply to the case $K_0 \cong 1$. When neutrinos become crowded, however, the phase space becomes enlarged in the radial orbit direction, giving $K_0 \ll 1$. The region where the density maximum occurs moves away from the center to a spherical shell. Consequently, the halo can contain more mass than its isotropic counterpart with the same maximum phase-space density. A revised phase-space mass bound is obtained. In the conservative case where neutrino velocities are comparable to stellar ones, the bound (3) becomes

$$m \gtrsim K_0^{1/4} m_{\rm TG} = K_0^{1/4}(120\ {\rm eV})\left(\frac{100\ {\rm km\ s^{-1}}}{\sigma}\right)\left(\frac{1\ {\rm kpc}}{r_c}\right)^{1/2} g_\nu^{-1/4}.$$

The upshot is that small neutrino mass implies $K_0 \ll 1$.

5. It is difficult to distinguish a hollow halo from a solid one on the basis of rotational velocity curves. This is shown in Figures 6 and 7. The central density region, which constitutes only a small volume, is not very important in determining the enclosed mass for velocity curves except in the rather problematic "core" region.

6. A number of questions arise. We have not considered the possibilities of three mass scales for three neutrinos. If the lightest neutrinos are relevant, could these lead to distinctly new dark matter objects? We have not discussed the probability of anisotropic halo formation. Could one phrase this as an effective probability distribution of the values of K_0? Small anisotropic objects are not very rare (Melott 1983), but much more study with high resolution is needed to come to any conclusions on the statistical likelihood of hollow halos. Perhaps two-dimensional simulations will offer sufficient statistics and resolution (Melott and Shandarin 1989).

It is interesting to speculate on the observational consequences of hollow neutrino halos. For small objects such as dwarf galaxies, it is possible that uncertainties in the visible matter distribution will make the hollowness or nonhollowness of a halo difficult to ascertain. A very large hollow halo might be observable in association with a galactic disk. The disk will be stabilized as usual outside the core region, but stars and gas could be unusually disorganized inside the core region. Is the Sombrero galaxy (NGC 4954) (Bajaja *et al.* 1984) an example of a large hollow halo? This is speculative and requires further study. How do we know for sure that the dark matter in our own or other spiral galaxies is not in a hollow halo?

The number of coincidences indicating neutrino dark matter has increased. Besides providing a natural explanation for the overall flatness of the universe, the size of a galaxy can be obtained from $K_0 \sim 1$; smaller, dwarf galaxy–like objects apparently come from $K_0 \ll 1$.

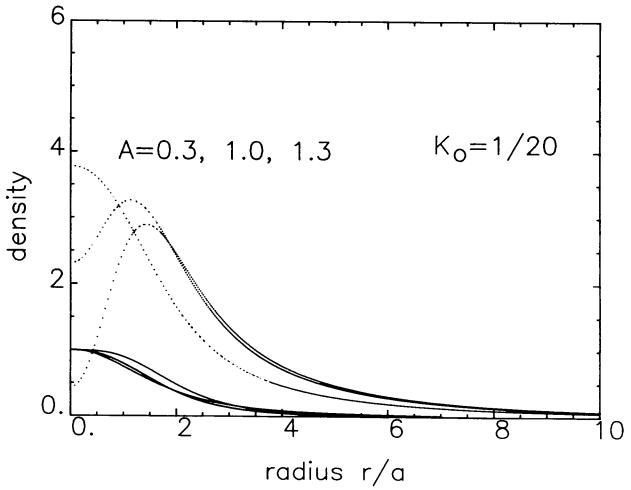

FIG. 7.—Comparison of isothermal distribution of stars or gas dominated by the dark matter density scaled by its central value: $n_g(r)/n_g(0)$. The curves are barely distinguishable for hollow or nonhollow halos [larger A gives smaller $n_g(r)$ for $r/a \gg 1$]. Upper curves (*dotted*) show the dark matter density for comparison.

We thank Adrian Melott and Sergei Shandarin for useful comments, and Richard Hamel for constructive help. This work was supported in part by Department of Energy grants DE-FG02-85ER40214.A005 and DE-FG02-85ER40214.A006 and University of Kansas General Research Fund grant 3714-0038.

REFERENCES

Aaronson, M. 1983, *Ap. J. (Letters)*, **266**, L11.
Antonov, V. A. 1962, *Vestnik Leningrad Univ.*, **7**, 135 (English transl. in *IAU Symposium 113, Dynamics of Star Clusters*, ed. J. Goodman and P. Hut [Dordrecht: Reidel]).
Bajaja, E., van der Berg, G., Faber, S. M., Gallagher, J. S., Knapp, G. R., and Shane, W. W. 1984, *Astr. Ap.*, **141**, 309.
Barnes, J. 1986, in *IAU Symposium 113, Dynamics of Star Clusters*, ed. J. Goodman and P. Hut (Dordrecht: Reidel), p. 297.
Binney, J. 1982, in *12th Advanced Course, Saas-Fée, Morphology and Dynamics of Galaxies*, ed. J. Binney, J. Kormendy, and S. D. M. White (Sauverny: Geneva Observatory).
Binney, J., and Tremaine, S. 1987, *Galactic Dynamics* (Princeton: Princeton University Press).
Carignan, C., and Freeman, K. C. 1988, *Ap. J. (Letters)*, **332**, L33.
Collins, C. A., Joseph, R. D., and Robertson, N. A. 1985, *Nature*, **320**, 506.
Cowsik, R. and Ghosh, P. 1986, *J. Ap. Astr.*, **9**, 7.
———. 1987, *Ap. J.*, **317**, 26.
Cowsik, R. and McClelland, J. 1972, *Phys. Rev. Letters*, **29**, 669.
———. 1973, *Ap. J.*, **180**, 7.
Davis, M., Lecar, M., Pryor, C. and Witten, E. 1980, *Ap. J.*, **250**, 423.
DeRujula, A., and Glashow, S. 1980, *Phys. Rev. Letters*, **45**, 442.
Dobyns, L. 1988, *Ap. J. (Letters)*, **329**, L21.
Doroshkevich, A. G., Zel'dovich, Ya. B., Sunyaev, R. A., and Klopov, M. Yu. 1980, *Soviet Astr. Letters*, **6**, 252.
Fridman, A. M., and Polyachenko, V. I. 1984, *Physics of Self-gravitating Systems* (Berlin: Springer).
Gell-Mann, M., Ramond, P., and Slansky, R. 1980, in *Supergravity*, ed. P. van Nieuwenhuizen and D. Freedmann (Amsterdam: North-Holland).
Kaiser, N. 1983, *Ap. J. (Letters)*, **273**, L17.
Kent, S. M., and Gunn, J. E. 1982, *A.J.*, **87**, 945.
Kormendy, J. 1985, in *IAU Symposium 117, Dark Matter in the Universe*, ed. J. Kormendy and G. R. Knapp (Dordrecht: Reidel), p. 139.
Kuhn, J., and Miller, R. H. 1989, *Ap. J. (Letters)*, **341**, L41.
Lin, D. N., and Faber, S. 1983, *Ap. J. (Letters)*, **266**, L21.
Lynden-Bell, D. 1979, *M.N.R.A.S.*, **187**, 101.
Madsen, J. 1989, University of Aarhus preprint.
Madsen, J., and Epstein, R. 1984, *Ap. J.*, **282**, 11.
Madsen, J., and Epstein, R. 1985, *Phys. Rev. Letters*, **54**, 2720.
McKay, D. W., and Ralston, J. P. 1989, in *Neutrino 88: Neutrino Physics and Astrophysics*, ed. J. Schneps, T. Kafka, W. A. Mann, and P. Nath (Singapore: World Scientific).
Melott, A. L. 1983, *Ap. J.*, **264**, 59.
———. 1985, *Ap. J.*, **289**, 2.
Melott, A. L., McKay, D. W., and Ralston, J. P. 1988, *Ap. J. (Letters)*, **324**, L43.
Melott, A. L., and Shandarin, S. 1989, *Ap. J.*, **343**, 26.
Merritt, D., and Aguilar, L. A. 1985, *M.N.R.A.S.*, **217**, 787.
Michie, R. W. 1963, *M.N.R.A.S.*, **125**, 127.
Palmer, P. L., and Papaloizou, J. 1987, *M.N.R.A.S.*, **224**, 1043.
Particle Data Group. 1988, *Phys. Letters B*, **204**, 136.
Ralston, J. P. 1989, *Phys. Rev. Letters*, **63**, 1038.
Ralston, J. P., and McKay, D. W. 1989, in *Particle Astrophysics: Forefront Experimental Issues*, ed. E. B. Norman (Singapore: World Scientific).
Ralston, J. P., McKay, D. W., and Melott, A. L. 1988, *Phys. Letters B*, **202**, 40.
Reynolds, R. J. 1984, *Ap. J.*, **282**, 191.
Reynolds, R. J., Magee, K., Roesler, F. L., Scherb, F. and Harlander, J. H. 1986, *Ap. J. (Letters)*, **309**, L9.
Rubin, V. 1985, in *IAU Symposium 117, Dark Matter in the Universe*, ed. J. Kormendy and G. R. Knapp (Dordrecht: Reidel), p. 51.
Scherrer, R. J., Melott, A. L., and Bertschinger, E. 1989, *Phys. Rev. Letters*, **62**, 379.
Schramm, D. and Steigman, G. 1981, *Ap. J.*, **243**, 1.
Sciama, D. W. 1989, *SISSA* preprint, No. 119.
———. 1990, in *Proc. Neutrino 90, Neutrino Physics and Astrophysics*, ed. J. Ellis *et al.* (Singapore: World Scientific), in press.
Silk, J. 1985, in *IAU Symposium 117, Dark Matter in the Universe*, ed. J. Kormendy and G. R. Knapp (Dordrecht: Reidel), p. 335.
Songaila, A., Bryant, W., and Cowie, L. 1989, *Ap. J. (Letters)*, **345**, L71.
Spergel, D. N., Weinberg, D. H., and Gott, J. R., III. 1988, *Phys. Rev. D*, **38**, 2014.
Stecker, F. W. 1980, *Phys. Rev. Letters*, **45**, 1460.
Tremaine, S., and Gunn, J. E. 1979, *Phys. Rev. Letters*, **42**, 407.
White, S. D. M., Frenk, C. S., and Davis, M. 1983, *Ap. J. (Letters)*, **274**, L1.
Yanagida, T. 1979, in *Proc. Workshop on Unified Theory and Baryon Number in the Universe*, ed. O. Sawada and A. Sugamoto.

JOHN P. RALSTON and LESLEY L. SMITH: Department of Physics and Astronomy, 1082 Malott Hall, University of Kansas, Lawrence, KS 66045